Research Square

Preprints are preliminary reports that have not undergone peer review.
They should not be considered conclusive, used to inform clinical practice,
or referenced by the media as validated information.

The thermal characteristics and performance indicators of energy-saving building envelope structures containing phase change materials

Yingjie Ma
Chongqing University
Keai Tao
Chongqing University
Jing Li
lj202740@cqu.edu.cn
Chongqing University
Yandong Wang
Chongqing University
Jiawei Huang
Chongqing University
Da Wang
Chongqing University
Hongquan Chen
Chongqing University
Shanshan Chen
Chongqing University
Kuan Sun
Chongqing University

Article

Keywords: Phase change material, Phase change energy storage gypsum board, Thermal regulation, Building energy conservation

Posted Date: August 12th, 2026

DOI: https://doi.org/10.21203/rs.3.rs-10379724/v1

License: This work is licensed under a Creative Commons Attribution 4.0 International License.
Read Full License

Additional Declarations: No competing interests reported.

The thermal characteristics and performance indicators of energy-saving building envelope structures containing phase change materials

Abstract: To enhance the thermal storage and temperature regulation capacity of building envelopes and reduce indoor temperature fluctuations, sandwich-type phase change gypsum boards were prepared using the sandwich method, and their thermal regulation performance was investigated through heat transfer experiments combined with COMSOL numerical simulation. Using palmitic acid–lauric acid eutectic composite phase change material as the functional layer, phase change gypsum boards with a sandwich thickness of 1 cm and dimensions of 10 × 10 × 3 cm^3 were fabricated. The results show that, compared with ordinary gypsum boards, the phase change gypsum boards exhibit significant peak-shaving and delayed heat transfer effects: the indoor-side temperature peak decreased from 32.43 °C to 31.17 °C, the inner wall-side temperature peak decreased from 39.90 °C to 34.91 °C, and the thermal lag time was extended by approximately 81 min. The 72 h transient heat transfer simulation results are consistent with the experimental trends. The phase change wall demonstrates lower overall temperature levels, smaller fluctuation amplitudes, more uniform indoor temperature field distribution, and more pronounced suppression of indoor temperature peaks during high-temperature periods. This study demonstrates that sandwich-type phase change gypsum boards can effectively enhance the thermal inertia of building envelopes, improve dynamic thermal performance, and possess promising application potential in the field of building energy conservation.

Highlights:

1.Sandwich-type phase change gypsum boards were prepared using a eutectic fatty acid composite phase change material as the functional layer.

2.The phase change boards reduced the indoor-side peak temperature by 1.26 °C and the inner wall-side peak by 4.99 °C, with a thermal lag of approximately 81 min.

3.Numerical simulations confirm that the PCM layer creates a thermal buffer that attenuates external disturbances, improves temperature field uniformity, and enhances the thermal inertia of building envelopes.

Key words: Phase change material; Phase change energy storage gypsum board; Thermal regulation; Building energy conservation

1 Introduction

With the continuous expansion of building scale and the increasing requirements for indoor thermal environments, building operational energy consumption has maintained a high proportion in global energy consumption[1, 2]. As the primary interface for heat exchange between buildings and the external environment, the thermal performance of building envelopes directly affects indoor temperature stability and building energy consumption levels. Although traditional wall materials possess certain advantages in structural load-bearing, durability, and basic thermal insulation, their thermal regulation mechanisms primarily rely on sensible heat storage and thermal resistance. Under periodic external temperature fluctuations, they often fail to effectively suppress indoor temperature peaks or actively regulate heat transfer

processes [3, 4]. Therefore, developing new envelope materials with thermal storage, peak-shaving, and delayed heat transfer capabilities has become an important research direction in building energy conservation [5, 6].

Phase change materials (PCMs) possess the characteristic of isothermal melting and solidification, enabling large-scale energy storage and release during phase transitions. Meanwhile, PCMs, with their high latent heat of fusion, have become excellent green energy storage carriers with promising applications in energy efficiency and ecological environmental protection [7-10]. Organic PCMs such as paraffin and fatty acids exhibit excellent latent heat storage performance and are commonly applied in building energy storage and textile temperature control; inorganic PCMs such as hydrated salts and metals possess higher thermal conductivity and are mostly used for electronic device cooling and packaging processes; bio-based PCMs prepared from renewable resources have been gradually promoted in environmentally friendly packaging and building substrates. In terms of regional applications, PCMs have achieved widespread adoption in North America, Europe, China, India, Japan, and South Asia. Furthermore, this material plays a critical role in numerous global industrial sectors including automotive and aerospace, fully demonstrating its application universality and popular characteristics [11-13]. Integrating PCMs with traditional building materials allows for the storage of solar energy and off-peak electricity when needed, thereby more effectively addressing the imbalance between thermal energy supply and demand [14-17]. Thermal energy storage, as the core fundamental substance

of renewable energy systems, improves thermal energy efficiency and has been extensively explored and widely applied in numerous studies [18-22].

Integrating PCMs with traditional building materials can store solar energy and off-peak electricity when needed, thereby more effectively resolving the imbalance between thermal energy supply and demand [23]. PCMs can be classified into three major categories: organic, inorganic, and eutectic[8, 22]. Due to their significant heat storage density, these materials possess the ability to store or release heat at nearly constant temperatures [24]. As isothermal heat storage media, PCMs have attracted researchers' attention for their application in building envelopes to reduce indoor temperatures and energy consumption [14, 25-30].

In recent years, extensive research has explored the integration of PCMs into building materials, particularly bricks—the most common building material—to evaluate their impact on thermal performance [31-37]. PCMs can be incorporated into bricks through three different methods: shape stabilization, filling PCMs into brick cavities, or encapsulation. Jia et al. [38] conducted a study to investigate the effect of incorporating PCM into sintered hollow bricks on improving wall thermal performance. The results showed that integrating PCM into hollow bricks could enhance the thermal inertia of walls. This had a significant impact on reducing the maximum heat flux on the inner surface, with peak heat flux decreasing from 38.7–35.2 W/m² to 19.2–26.1 W/m², a reduction of 50%. Abbas et al. [39] performed experimental and simulation evaluations of PCM application in Iraqi hollow bricks, achieving a 4.7 °C reduction in indoor temperature, an average fluctuation of 23.84%, and a delay increase of 2 hours.

In Mediterranean cities, optimal energy savings of approximately 56% were observed through the use of PCM hollow bricks in wall construction [34]. Jin et al. [40] concluded that the thermal properties of PCM and its surrounding environment affect the optimal location for implanting a PCM layer in walls. In another study [41], the inner surface temperature increased. The PCM layer is expected to be positioned close to this location. The explanation is that, compared with other locations, this position allows the PCM to collect and release latent heat throughout the entire thermal cycle. Kabdrakhmanova et al. [42]modeled humid subtropical environments across multiple cities using a mid-rise four-story residential building, demonstrating annual energy savings of 12,635 kWh, a 19.9% reduction in energy use; nevertheless, atmospheric pressure, solar azimuth angle, and wind speed still exerted influence on energy consumption. PCM-bricks show promise for building energy efficiency, yet key issues remain: climate-dependent design, cycling stability, leakage, low thermal conductivity, and unclear economic viability. Future efforts should address these through integrated material and system optimization.

Among numerous building substrates, gypsum boards have become one of the important carriers for PCM composite applications due to their mature molding processes, low cost, convenient construction, and easy integration with building envelopes. Based on this, this study adopts the sandwich method to prepare phase change gypsum boards, using montmorillonite/palmitic acid–lauric acid composite phase change materials (CPCMs) as the functional layer, and systematically investigates their thermal regulation performance. First, comparative experiments were

conducted to analyze the temperature response differences between phase change gypsum boards and ordinary gypsum boards during heating and cooling processes, and thermal lag tests were performed to evaluate their delayed heat transfer capability. Subsequently, based on COMSOL Multiphysics, transient heat transfer models for phase change walls and ordinary walls were established, and numerical simulations of temperature variation patterns and temperature field distribution characteristics under 72 h conditions were conducted for building models. Finally, from both experimental and simulation perspectives, the mechanisms of sandwich-type phase change gypsum boards in peak-shaving, lagging, and stabilizing indoor thermal environments were revealed, providing theoretical basis and experimental support for their application in building energy-saving envelopes.

2 Experimental study on preparation of sandwich-type phase change gypsum boards

2.1 Preparation of Composite Phase Change Materials

The sandwich-type phase change functional material used in this study is montmorillonite-supported palmitic acid–lauric acid composite phase change material (MMT/PA-LA). Among these, PA-LA is a palmitic acid–lauric acid binary eutectic fatty acid system serving as the phase change matrix, which exhibits stable solid–liquid phase change behavior and high phase change latent heat within the suitable building temperature range, enabling efficient heat absorption and release during phase transitions to achieve temporal redistribution of heat. MMT is KH550 (3-

aminopropyltriethoxysilane, γ-aminopropyltriethoxysilane) surface-modified montmorillonite serving as a porous adsorption carrier, which loads and encapsulates the PA-LA phase change matrix, effectively suppressing liquid fatty acid leakage during phase transitions and improving the shape stability, thermal cycling reliability, and structural integrity of CPCMs.

Through carrier loading and interface modification, MMT/PA-LA composite phase change materials possess both high latent heat storage characteristics and excellent shape stability. The phase change temperature matches the indoor thermal regulation requirements of buildings, making it suitable as a sandwich functional layer embedded in gypsum board structures, providing stable and long-lasting thermal regulation capability for phase change gypsum boards.

2.2 Thermal Performance Analysis of Composite Phase Change Materials

The DSC curves in Fig. 1 reveal that pure PA-LA and its composites all exhibit distinct solid–liquid phase-change endothermic and exothermic peaks within 25–40 °C, confirming that PA-LA maintains reversible thermal storage capability after compositing. Compared with pure PA-LA, MMT/PA-LA and KH550-MMT/PA-LA show reduced peak intensities, broadened peaks, and shifted peak positions, attributable to pore confinement and interfacial interactions that cause dispersed crystallization/melting behaviors of PA-LA molecules, reducing the effective

proportion participating in phase transitions, while the confinement effect also adjusts the phase-change temperature range by altering nucleation barriers and undercooling.

Further comparison reveals that the KH550-modified MMT composite exhibits more regular peak shapes and a more concentrated temperature range, closely approaching the single-peak behavior of pure PA-LA, indicating that surface modification improves interfacial compatibility and PCM distribution uniformity, thereby maintaining higher crystallinity and reversibility while suppressing leakage. Overall, the shape-stabilized composite strategy effectively encapsulates PA-LA but somewhat reduces latent heat storage density; surface modification offers a better balance between leakage prevention and phase-change performance.

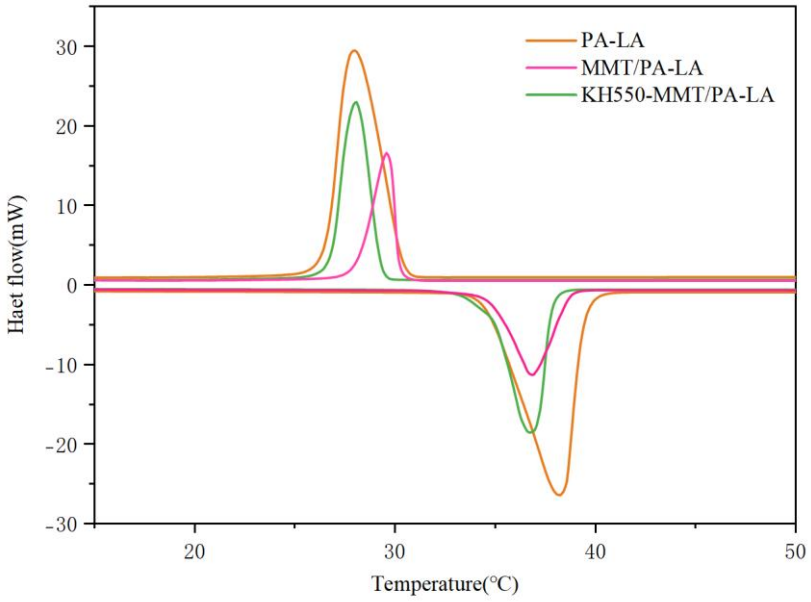


Fig. 1. DSC curves of PA-LA, MMT/PA-LA, and KH550-MMT/PA-LA

The TG-DTG curves in Fig. 2 characterize the thermal decomposition processes and weight loss rate differences of MMT/PA-LA and KH550-MMT/PA-LA. Both TG curves exhibit typical patterns of low-temperature slow weight loss, medium-

temperature rapid weight loss, and high-temperature residual stability. The low-temperature segment shows only slight weight loss, primarily from the removal of adsorbed water or weakly bound volatile components, indicating mass stability within commonly used building temperature ranges. The medium-temperature region is the main weight loss stage, with DTG showing a main peak near approximately 300 °C, corresponding to the rapid pyrolysis and volatilization of organic phase PA-LA and a small amount of organic modification groups. The high-temperature segment curves tend to flatten and form stable residuals, with residuals primarily from the montmorillonite inorganic skeleton, indicating good high-temperature structural stability of the system.

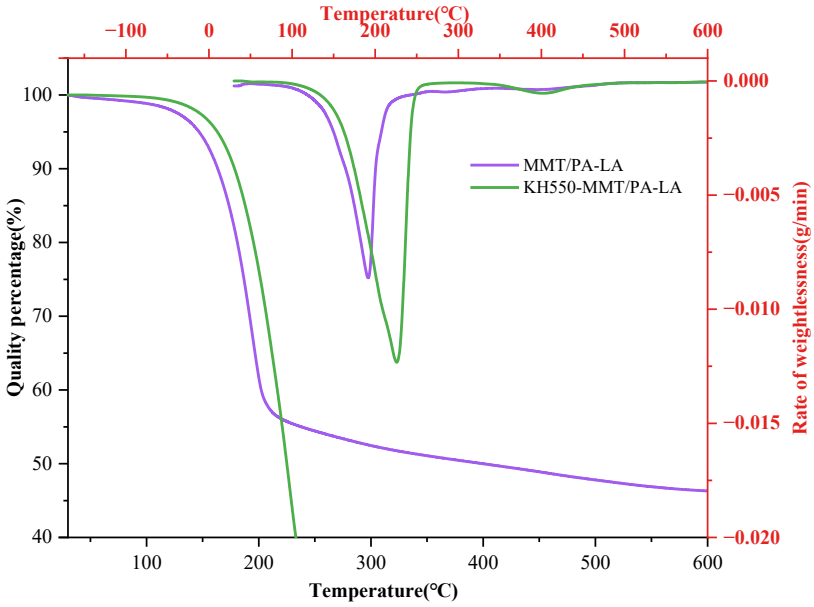


Fig. 2. TG-DTG curves of MMT/PA-LA and KH550-MMT/PA-LA composites

The DSC curves in Fig. 3 are used to compare the thermal response characteristics of PA-LA and its state after 200 thermal cycles, and further evaluate the maintenance degree of phase change behavior before and after cycling of the KH550-MMT/PA-LA

composite phase change system, thereby characterizing the material's thermal cycling durability and phase change stability. All four sample groups exhibit clear endothermic and exothermic peaks in the approximately 27–40 °C range, indicating that both pure PA-LA and composite systems maintain basic solid–liquid phase change reversibility after thermal cycling, demonstrating good phase change functional sustainability.

From the perspective of phase change temperature repeatability, pure PA-LA shows a certain degree of peak position shift in melting and crystallization peaks after 200 cycles compared with initial samples, accompanied by peak shape evolution from sharp to broadened, indicating that thermal cycling may cause crystal morphology reconstruction, crystal defect accumulation, or component micro-rearrangement, leading to adjustments in crystallization kinetic pathways and undercooling behavior, causing drift in phase transition temperature ranges and dispersion of phase transition processes. In contrast, the curves of KH550-MMT/PA-LA after 200 cycles are highly similar to the initial composite samples, with smaller peak position changes and relatively regular peak shapes maintained. This indicates that the carrier's confinement effect and interface interactions provide stable anchoring and constraint effects on PA-LA molecules during cycling, effectively suppressing migration, leakage, and macroscopic phase separation of molten-state molecules, thereby improving the repeatability and consistency of phase change temperature and phase transition processes.

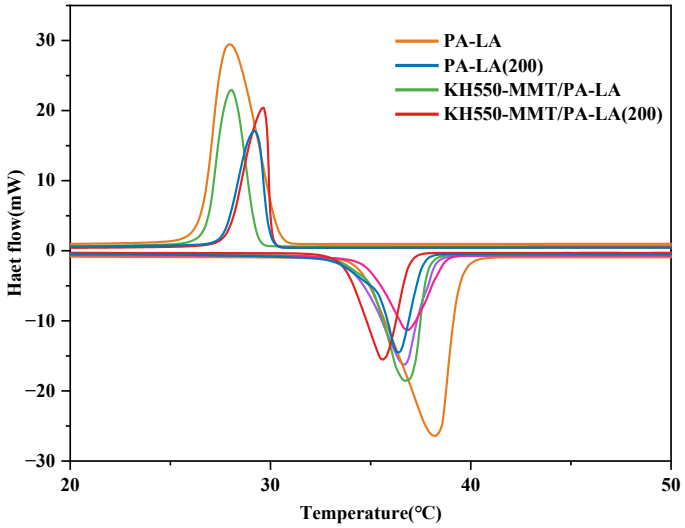


Fig. 3. DSC curves of PA-LA and KH550-MMT/PA-LA composites before and after thermal cycling

To further improve the phase change reversibility and thermal cycling reliability of fatty acid phase change materials, optimization can be conducted from the perspective of crystallization kinetics regulation [43]. By introducing trace nucleating agents or crystal form regulators, the probability of heterogeneous nucleation can be increased, undercooling can be reduced, and phase transition path drift caused by polymorphic transitions can be suppressed [44], thereby alleviating DSC peak broadening and peak position shifts during cycling and enhancing phase change peak reversibility.

2.3 Preparation of phase change gypsum boards

Fig. 4 illustrates the specific preparation process of sandwich-type phase change gypsum boards in this study is as follows: First, a mold with specifications of 10 cm × 10 cm × 3 cm was prepared. Demolding agent was evenly applied to the inner walls of

the mold to facilitate subsequent demolding. Then, a certain mass of building gypsum powder was weighed and thoroughly mixed at a water-gypsum ratio of 0.48. The prepared gypsum slurry was poured into the mold to prepare gypsum boards with a thickness of 1 cm. After initial hardening of this gypsum board, an 8 cm × 8 cm × 2 cm foam frame was placed in the center position. Gypsum slurry was poured into the mold again to form gypsum boards with hollow structures. After the gypsum slurry reached the initial setting state, the pre-placed foam frame was removed. The formed cavity was filled with CPCMs, with the phase change layer thickness controlled at 1 cm. Subsequently, gypsum slurry was re-prepared, poured into the remaining space of the mold, and the surface was leveled with a scraper. Finally, phase change gypsum boards with dimensions of 10 cm × 10 cm × 3 cm and sandwich thickness of 1 cm were obtained. After complete hardening, the samples were demolded and placed in a 40 °C blast drying oven until mass stabilization, as shown in Fig. 5, then reserved for testing. As controls, ordinary gypsum boards and phase change gypsum boards were simultaneously prepared in this experiment, designated as CPCM1 and CPCM2 respectively.

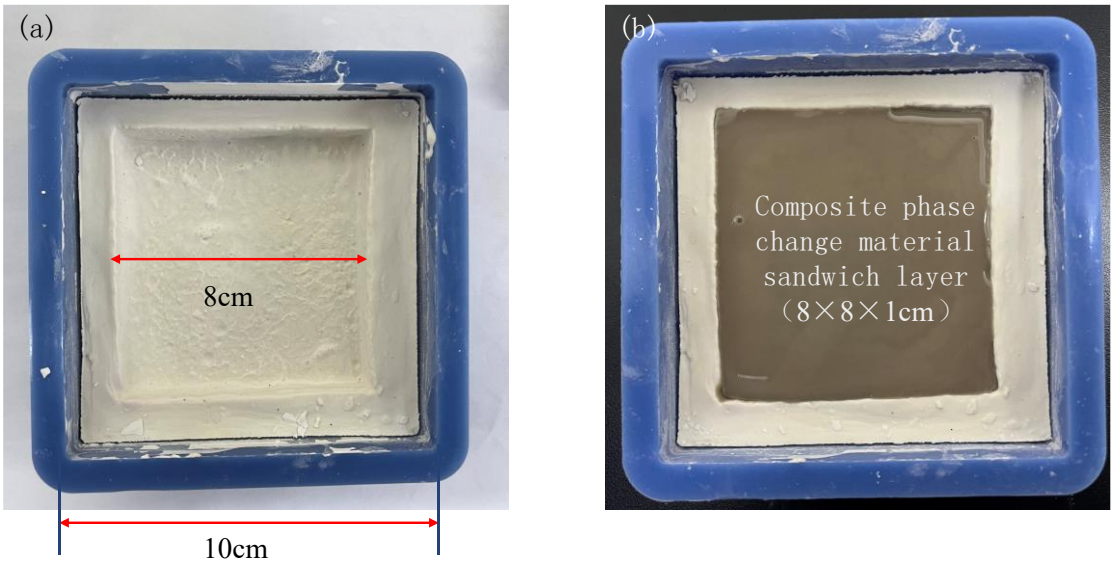


Fig. 4. Photographs of the preparation process of sandwich-type phase change gypsum board: (a) hollow-structure gypsum board; (b) sandwich gypsum board filled with composite phase change material

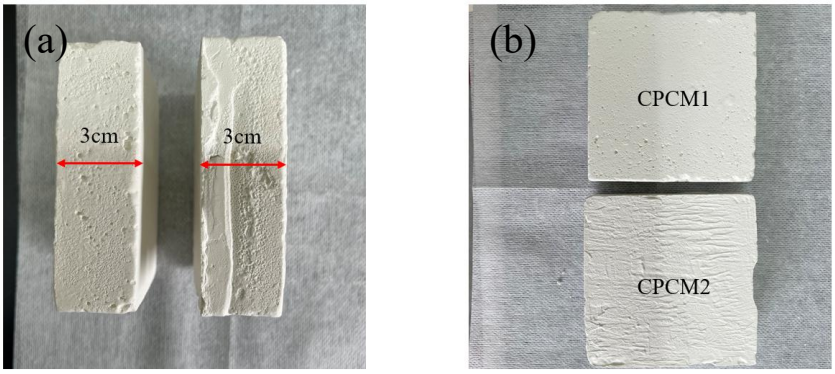


Fig. 5. Photographs of different composite phase change gypsum board samples: (a) schematic view of sample thickness; (b) comparison of surface conditions of CPCM1 and CPCM2

2.4 Heat Transfer Performance Testing of Sandwich-Type Phase Change Gypsum Boards

To verify the thermal insulation characteristics of phase change gypsum boards, two specification-consistent simulated rooms were constructed in this study ,as shown in Fig. 6. The internal dimensions of both simulated rooms were length × width × height = 25 cm × 25 cm × 30 cm. One simulated room was enclosed with five EPS insulation boards and one blank gypsum board as the control group; the other simulated room was enclosed with five EPS insulation boards and one phase change energy storage gypsum board as the experimental group.



Fig. 6. Photographs of the comparative experimental models of the phase change wall and ordinary wall: (a) phase change wall; (b) ordinary wall; (c) overall structure of the experimental model

Fig. 7 shows the temperature control performance testing of phase change gypsum boards adopted a laboratory self-made testing device, which mainly consists of two core components: the simulated room and the external heat source. Fig. 8 simultaneously presents a three-dimensional structural schematic of this device, clearly showing the overall construction. To comprehensively and accurately collect temperature data inside

the simulated room, four temperature sensors were reasonably arranged inside the simulated room. All sensors were connected to a temperature controller to achieve real-time transmission and recording of temperature data. A 250 W heat source was installed at a fixed position on the outer side of the testing device to provide stable and controllable heat load for the testing process, ensuring consistency of testing conditions. The specific steps for temperature control performance testing are as follows: First, the entire testing device was placed in a 20 °C constant temperature environment and allowed to stand until temperatures at all parts of the device reached stable states. Then, the external heat source was turned on to continuously heat the simulated room. After the heating process was completed, the device was maintained in the 20 °C constant temperature environment for natural cooling. Throughout the heating and cooling processes, temperature data inside the simulated room was collected and recorded by a temperature recorder throughout the entire process, and complete heating and cooling curves were plotted. Based on these curves, the temperature control effectiveness of phase change gypsum boards was systematically analyzed.



Fig. 7. Photograph of the light-heating heat transfer test setup for the wall model

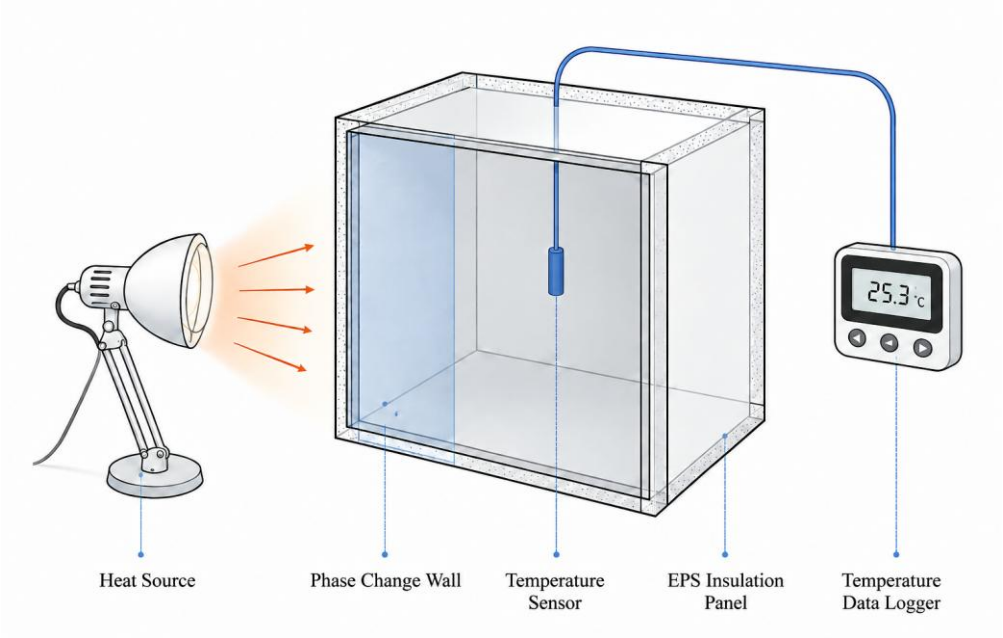


Fig. 8. Schematic diagram of the heat transfer performance test setup for the phase change wall

Based on the test curves in Fig. 9, compared with ordinary gypsum board walls, sandwich-type phase change energy storage gypsum board walls demonstrate superior thermal regulation performance on both the indoor side and inner wall side. This phenomenon directly confirms that the phase change layer with PA-LA as the matrix can play a significant heat storage buffering role in the wall heat transfer process. The overall thermal response characteristics of the two differ significantly. Ordinary gypsum board walls heat up rapidly during the heating stage, with temperature peaks appearing earlier, followed by rapid entry into the cooling stage. Sandwich-type phase change energy storage gypsum board walls exhibit a more gradual temperature variation trend, with not only significantly reduced temperature peaks and delayed peak occurrence times, but also more moderate temperature attenuation amplitudes during the cooling stage, highlighting their peak-shaving, valley-filling, and delayed heat transfer effects on heat transfer.

From the temperature variation curves throughout the entire test cycle, it can also be observed that the temperature fluctuation amplitude of phase change energy storage gypsum board walls is overall smaller than that of ordinary gypsum board walls, indicating that sandwich-type phase change gypsum boards can effectively improve wall thermal stability. The core mechanism lies in that PCM, through phase change latent heat effects, performs staged heat absorption and re-release on heat flow, achieving temporal redistribution of heat, thereby weakening the instantaneous response of walls to external thermal disturbances. Especially under scenarios with large daytime heat loads, this heat absorption peak-shaving and heat release delay mechanism can effectively improve the transient heat transfer performance of walls, enabling building envelopes to maintain more stable temperature responses in dynamic thermal environments.

Focusing on indoor temperature response, the indoor peak of ordinary gypsum board walls is approximately 32.43 °C, while the sandwich-type phase change energy storage gypsum board reduces it to 31.17 °C, with a peak reduction of 1.26 °C and slightly delayed peak occurrence time. This indicates that the phase change layer can absorb part of the heat during heat transfer from outdoor to indoor, reduce indoor heat flux density, thereby suppressing rapid room temperature rise and slowing heat accumulation during high-temperature periods, improving indoor thermal environment stability. Compared with the indoor side, the inner wall side temperature regulation effect is more significant: the inner wall side peak of ordinary gypsum board is approximately 39.90 °C, while the phase change gypsum board reduces it to 34.91 °C,

a decrease of 4.99 °C, with further delayed peak occurrence time. This indicates that the phase change layer has a more direct inhibitory effect on concentrated heat transfer within the wall, can delay heat penetration through the wall, and enhance envelope thermal inertia; the significant reduction in inner wall side peak also means weakened heat storage on the inner wall surface, reducing secondary heat release to the indoor environment, which is beneficial for improving thermal insulation performance.

The above differences mainly originate from the latent heat absorption and release behavior of PA-LA eutectic fatty acids within the phase change temperature range. When external thermal effects intensify, the sandwich PCM gradually undergoes solid–liquid phase transition and absorbs large amounts of latent heat, causing part of the input heat to be stored as latent heat rather than converted to sensible heat, thereby reducing temperature peaks and delaying peak occurrence. After external temperature decreases, the melted PCM slowly solidifies and releases latent heat, making the temperature attenuation during the cooling stage more gradual. The overall curves further show that phase change wall temperature fluctuation amplitudes are smaller than ordinary walls, reflecting their temporal redistribution of heat through staged heat absorption and delayed heat release, thereby weakening the instantaneous influence of external thermal disturbances. Especially under conditions with large daytime heat loads, this peak-shaving, lagging, and slow-release mechanism can improve envelope transient heat transfer characteristics, making indoor temperature responses more stable and thermal comfort more enduring.

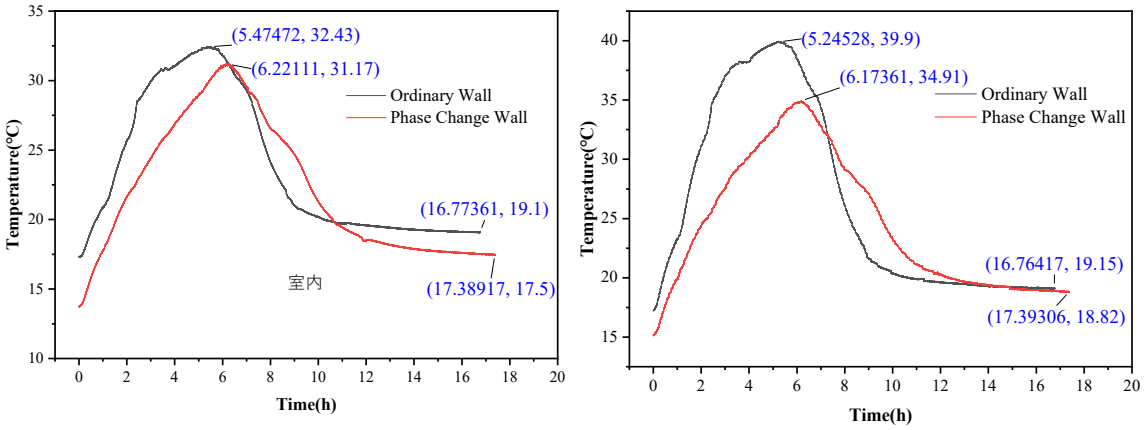


Fig. 9. Comparison of temperature response curves of the ordinary wall and phase change wall at the indoor side and inner wall side: (a) indoor side; (b) inner wall side

The interlayer phase change energy storage gypsum board has superior thermal regulation performance compared to ordinary gypsum board walls. Specifically, it shows a reduction in temperature peaks, a delay in the occurrence time of peaks, and a slowdown in the cooling process. The effect of reducing temperature peaks on the inner side of the wall is particularly significant, fully demonstrating the crucial role of the low-melting-point fatty acid phase change layer in the heat transfer path of the wall. This study confirms that applying PCM to the interlayer structure of gypsum boards can effectively enhance the heat storage capacity and thermal stability of the wall, and has positive theoretical and practical value for improving the thermal performance of building envelope structures.

2.5 Thermal Lag Test

To further complete the thermal performance evaluation of phase change gypsum boards, this study supplemented thermal lag tests. Thermal lag tests use temperature response as the evaluation benchmark, comparing the time differences required for

ordinary gypsum boards and phase change gypsum boards to reach predetermined temperatures under the same thermal conditions, to characterize the delay capability of phase change gypsum boards for heat transfer and their comprehensive heat storage and thermal insulation performance. Fig. 10 presents the temperature–time variation curves plotted with the testing device space temperature as reference. The test results clearly show that the temperature variation patterns of ordinary gypsum board walls and phase change gypsum board walls during the heating process differ significantly. Ordinary gypsum board walls heat up at a faster rate and can reach peak temperatures in a shorter time, while phase change gypsum board walls exhibit a relatively more gradual heating process, with significantly extended time required to reach peak temperatures, demonstrating prominent thermal lag characteristics. From the test data, it is clear that ordinary gypsum board walls reach the highest temperature of 32.42 °C at 12,819 s, while phase change gypsum board walls reach the highest temperature of 32.49 °C at 17,694 s. Although the peak temperatures of both are basically similar, the time for phase change gypsum board walls to reach peak temperature is delayed by approximately 81 min compared with ordinary gypsum board walls. This quantitative data intuitively confirms the significant delay effect of phase change gypsum boards on heat transfer during the heating process.

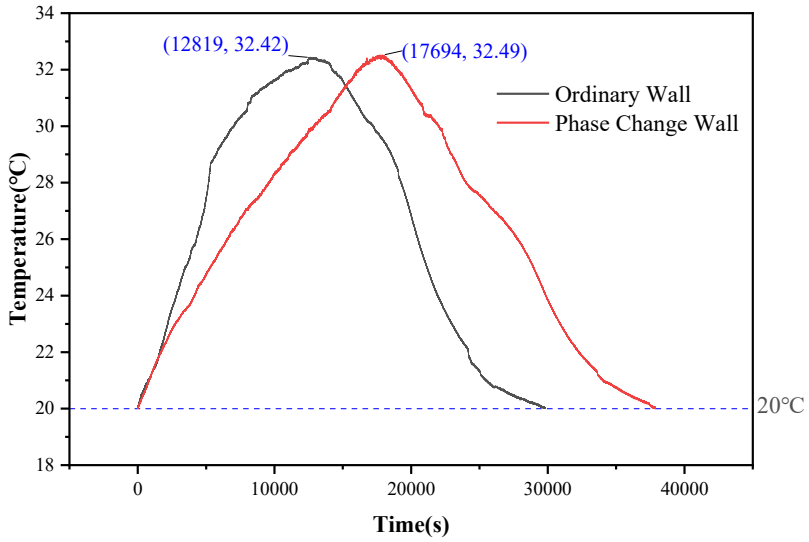


Fig. 10. Thermal lag test curves of ordinary gypsum board and phase change gypsum board

The generation of this thermal lag phenomenon is primarily due to the phase change reaction occurring in CPCMs within phase change gypsum boards during the heating process, simultaneously absorbing large amounts of latent heat. This causes part of the input heat to fail to immediately convert to sensible heat for raising material temperature, thereby reducing the temperature rise rate of phase change gypsum boards and extending the time required to reach predetermined temperatures. In contrast, ordinary gypsum boards rely solely on sensible heat for heat storage, with faster temperature response speeds, and therefore more rapid heating processes. Meanwhile, the test curves also show that the curve variation of phase change gypsum board walls during the cooling stage is more gradual, indicating that PCM can slowly release previously stored heat during the heat release process, effectively weakening temperature fluctuation amplitudes and further improving wall thermal stability. Phase change gypsum boards possess good heat storage, thermal insulation, and delayed heat

transfer performance. The enhancement of their thermal lag characteristics further improves the dynamic thermal performance of building envelopes, complementing the thermal regulation effectiveness described above, and fully validating the application value of sandwich-type phase change gypsum boards in building energy conservation.

2.6 Multi-Dimensional Performance Comparison Between Phase Change Composite Materials and Sintered Hollow Bricks

Table 1 based on the engineering properties and thermal mechanism of building envelope materials, conducts a multi-dimensional comparison between the fatty acid-based shape-stabilized composite phase change material prepared in this study and the sintered hollow bricks. The fatty acid-based shape-stabilized composite phase change material (PCM) prepared in this study differs significantly from sintered hollow bricks in functionality and thermal mechanism, and they are complementary. Sintered hollow bricks, as traditional masonry materials, offer advantages in load-bearing, durability, and mature construction, relying on cavity structures to increase thermal resistance for steady-state insulation. However, they rely solely on sensible heat storage and cannot form a latent-heat buffering platform within the target temperature range, resulting in limited peak suppression and response lag under periodic temperature fluctuations. In contrast, the composite PCM achieves a directional phase-transition temperature range via eutectic fatty acids, is shape-stabilized by porous carriers, and introduces latent-heat storage, enabling peak shaving during heating and delayed heat release during cooling, thereby reducing indoor temperature fluctuations and improving thermal comfort. Its

thermal conductivity can be enhanced by adding high-conductivity fillers to improve dynamic temperature regulation efficiency. In terms of safety, sintered bricks have no leakage or degradation issues, while the PCM composite needs attention to leakage, cycling stability, and fire safety, but these can be made engineering-controllable through shape-stabilized encapsulation and component verification.

In summary, sintered hollow bricks are more suitable as structural envelope substrates providing mechanical support and basic thermal resistance, while the phase change composite materials in this study are more suitable as functional layer sandwiches providing latent heat buffering and peak-shaving lagging effects in specific temperature ranges. Synergistic integration at the construction level can potentially significantly improve the dynamic thermal performance and indoor thermal environment stability of envelopes while maintaining masonry system reliability.

Table 1 Comparison of Key Properties between Phase Change Composites and Sintered Hollow Bricks

Comparison Dimension	Fatty Acid-based Composite Phase Change Material	Sintered Hollow Brick
Functional Positioning	Latent heat storage and temperature regulation within the temperature zone	Structural enclosure matrix
Temperature Regulation Mechanism	Solid-liquid phase change latent heat, enabling time redistribution of heat absorption, storage, and release	Sensible heat storage and thermal resistance

Comparison Dimension	Fatty Acid-based Composite Phase Change Material	Sintered Hollow Brick
Dynamic Thermal Response	Peak reduction, peak delay, and significant temperature fluctuation convergence	Primarily reduces heat flux; limited dynamic peak-shaving capability
Phase Change Temperature Zone	Customizable via eutectic ratio design	No phase change platform; temperature zone not customizable
Heat Transfer Capability	Intrinsically low; can be enhanced by thermally conductive fillers	Affected by porosity and moisture content; overall medium-low thermal conductivity
Leakage Risk	Requires shape-stabilized encapsulation and interface control to suppress leakage	No leakage issues
Mechanics & Construction	Needs integration with substrate; limited standalone load-bearing capacity	High compressive strength; mature construction system
Durability & Safety	Requires verification of thermal cycling stability and fireproofing design	Fire-resistant and weather-resistant; stable long-term service
Engineering Integration	Suitable for interlayers and functional layers embedded in walls or panels	Suitable for main masonry and infill wall materials

3 Numerical Simulation of Temperature Field in Composite Phase Change Concrete Building Model

To further verify the performance of phase change components at actual building scales, a phase change concrete wall building model was established based on COMSOL, and 72 h transient heat transfer numerical simulation was conducted.

The numerical simulation adopts three-dimensional modeling, selecting the phase change heat transfer submodule under the solid heat transfer module in single-physics field, with focus on studying transient temperature field variation characteristics. During simulation, external environmental temperature fluctuations are taken as the core influencing factor, with maintaining indoor temperature within the human comfort range (approximately 26 °C) as the control target. Through simulation analysis, the temperature regulation effect of composite phase change concrete on indoor temperature and the dynamic response patterns of the temperature field are clarified.

3.1 Phase Change Concrete Wall Model Establishment and Parameter Setting

A simplified three-dimensional concrete building model was constructed. The model consists of envelope walls and indoor air domain. The envelope structure is set to two conditions: phase change walls and ordinary concrete walls, for comparative analysis. The building exterior dimensions are 400 cm × 400 cm × 300 cm, with wall thickness uniformly taken as 30 cm. Therefore, the indoor air domain dimensions are 340 cm × 340 cm × 240 cm. The established geometric model is shown in Fig. 11. To

ensure comparability, except for whether the wall material contains phase change components, all other geometric dimensions and boundary conditions remain consistent.

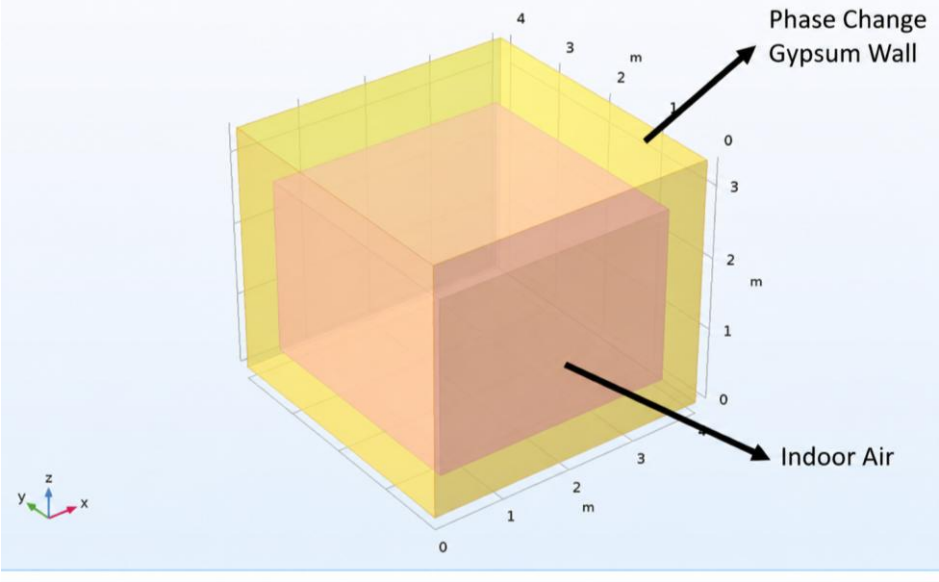


Fig. 11. Schematic diagram of the computational domain of the building model with phase change gypsum board

The phase change heat transfer submodule in the solid heat transfer module was selected to conduct wall transient heat transfer simulation. To highlight the dominant role of material thermal properties and phase change latent heat effects, and to reduce model complexity while ensuring calculation accuracy, the following reasonable assumptions were made during model establishment:

1)Wall materials and indoor air are considered homogeneous continuous media with isotropic thermal properties;

2)The influence of humidity and moisture migration on heat transfer processes is not considered;

3)Liquid phase natural convection and undercooling kinetic effects during PCM

melting and solidification processes are neglected;

4)Radiative heat transfer is neglected, considering only convective heat transfer driven by internal and external temperature differences and heat conduction within walls;

5)The heat transfer process mainly develops along the wall thickness direction, and the model is equivalently simplified to a one-dimensional transient heat transfer problem in calculation;

6)Except for phase change walls, thermal property parameters of materials in other domains are treated as constants.

In this numerical model, heat exchange between envelope structures and indoor/outdoor air is driven by temperature differences, mainly including heat conduction within walls and convective heat transfer between wall surfaces and air. Both jointly determine heat transfer along the path of external environment, walls, and indoor air. After introducing the phase change layer, walls can achieve staged heat storage and release through latent heat absorption and release during rapid external temperature fluctuations, equivalent to forming a thermal buffer, thereby weakening the transient response of indoor temperature to external disturbances, making indoor temperature changes more stable and maintained within relatively comfortable ranges. Required thermal property parameters for simulation include phase change temperature, phase change latent heat, density, thermal conductivity, and specific heat capacity, all prioritized using measured data from this study. Missing parts are supplemented through literature review with unified parameter sources and value ranges. To

quantitatively characterize temperature control effects, domain probes are arranged in the model to extract key indicators such as indoor average temperature, indoor maximum and minimum temperatures, and phase change wall average temperature, for subsequent temperature curve and temperature field comparative analysis. Material parameters are set in Table 2.

Table 2 Physical parameters of various materials of the model house

Material	Thermal Conductivity (W/(m·K))	Density (kg/m³)	Specific Heat at Constant Pressure (J/(kg·K))	Specific Heat Ratio	Phase Change Temperature (°C)	Phase Change Latent Heat (kJ/kg)
Ordinary concrete wall	1.28	2352	970	1	/	/
Phase change concrete wall (before phase change)	1.18	2100	2260	1.1	30	100
Phase change concrete wall (after phase change)	1	2100	4500	1	30	100

Air (software embedded)	0.023	1.29	1005	1.4	/	/

The temperature load q^* between wall temperature and external temperature, indoor temperature is described by Newton's cooling equation:

$$q^*=h_f(T_1-T_2) \tag{1}$$

Where, h_f is the convective heat transfer coefficient, W/(m²·K);T_1 is the solid surface temperature, °C; T_2 is the fluid temperature surrounding the solid, °C. The heat transfer process of the model wall is simplified to one-dimensional convective heat transfer, greatly simplifying calculations. The thermal conduction control equation can be expressed as:

$$\rho\frac{\partial H}{\partial t}=k_w\frac{\partial^2 T}{\partial x^2} \tag{2}$$

Where, ρ is the density of phase change concrete wall, kg/m³; H is the phase change enthalpy of phase change concrete wall, kJ/kg; t is time, s;k_w is the thermal conductivity of phase change concrete wall, W/(m·K); T is temperature, °C; x is the calculation step size, m. Assuming the external environmental temperature function curve is $y=8\,sin[(\pi/12)t]+30$. The function curve is shown in Fig. 12.

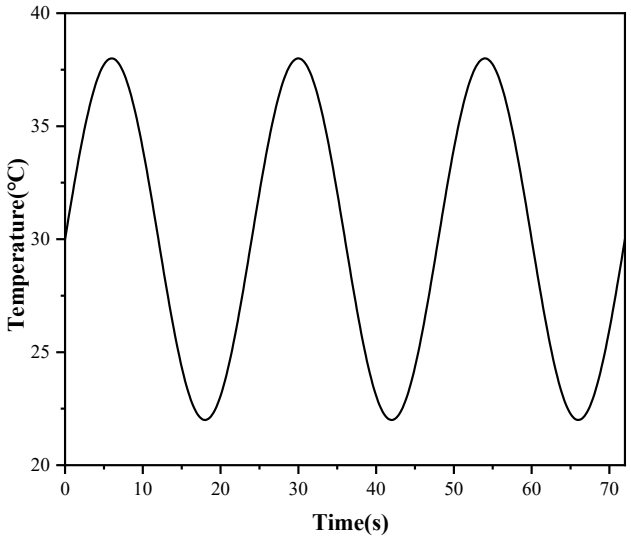


Fig. 12. Curve of the ambient environmental temperature function

In solid heat transfer, the research control governing equations are Equations 4 and 5:

$$\rho C_p \frac{\partial T}{\partial t} + \rho C_p u \cdot \nabla T + \nabla \cdot q = Q + Q_{ted} \tag{4}$$

$$q = -k\nabla T \tag{5}$$

Where, ρ is fluid density, kg/m³; C_p is heat capacity at constant pressure, J/(kg·K); T is temperature, K; u is velocity field, m/s; k is thermal conductivity, W/(m·K); Q is heat source, W/m³; calculated by mass and momentum conservation equations; q is heat flux, W/m².

The overall initial temperature is set to 26 °C, the indoor interface is set as an isothermal domain interface, and the convective heat transfer coefficient is set to 10 W/(m²·K). The research control governing equations are Equations 6 and 7.

$$-n \cdot q = 0 \tag{6}$$

$$q = h(T_{ext} - T) \tag{7}$$

Where, n is the boundary outward normal vector, T_{ext} is the external

environmental temperature (K). Since the phase change component in phase change concrete walls continuously evolves in solid–liquid phase ratio during melting and solidification processes, its equivalent thermal property parameters are not constants but change with liquid phase volume fraction. To more realistically characterize the nonlinear features of material thermal properties within the phase change interval, this study assigns and updates parameters such as density, specific heat capacity, and thermal conductivity of composite phase change concrete using piecewise weighted forms according to Equations 8 – 11, enabling the model to reflect the dynamic changes of thermal properties with phase state transitions during phase change processes.

$$\rho=\theta_1\rho_1+\theta_2\rho_2 \tag{8}$$

$$C_p=\frac{1}{\rho}\left(\theta_1\rho_1 C_{p,1}+\theta_2\rho_2 C_{p,2}\right)+H_{1\to 2}\frac{\partial\alpha_n}{\partial T} \tag{9}$$

$$k=\theta_1 k_1+\theta_2 k_2 \tag{10}$$

$$\theta_1+\theta_2=1 \tag{11}$$

Where, ρ is the density of composite phase change concrete, kg/m³; C_p is the specific heat capacity of composite phase change concrete, J/(kg·K); k is the thermal conductivity of composite phase change concrete, W/(m·K); H is the latent heat of composite phase change concrete, kJ/kg. Where, α_m can be expressed as $\alpha_m=(\theta_2\rho_2-\theta_1\rho_1)/2(2\theta_1\rho_1+\theta_2\rho_2)$.

The phase change temperature of CPCMs in the phase change concrete wall is set to 303.15 K, the phase transition interval is 1 [K], and the phase change latent heat is 100 kJ/kg. Since no forced ventilation is applied in the indoor space, air movement is mainly dominated by natural convection, where air forms buoyancy and induces flow

under gravity due to spatial density differences caused by temperature differences. Based on this, the indoor air domain in this study is set to a laminar flow model with the gravity term enabled to characterize buoyancy-driven effects. To improve numerical convergence of flow field solutions, a pressure reference point is introduced in the calculation domain, which can be arbitrarily selected within the indoor air domain, to eliminate rigid body degrees of freedom of the pressure field and stabilize the solution process. Indoor air physical property parameters adopt the COMSOL built-in material library. Flow governing equations use the incompressible Navier-Stokes equations (Equations 12 – 14), including momentum conservation and continuity equations:

$$\rho\frac{\partial u}{\partial t}+\rho(u\cdot\nabla)u=\nabla\cdot[-pI+K]+F+\rho g \tag{12}$$

$$\rho\nabla\cdot u=0 \tag{13}$$

$$K=\mu(\nabla u+(\nabla u)^T) \tag{14}$$

Where, ρ is fluid density, kg/m³; μ is fluid velocity field, m/s; p is fluid pressure, Pa; k is thermal conductivity, W/(m·K); F is volume force field, N/m³. Mesh division adopts a swept mesh strategy. The indoor air domain is set to extra fine mesh, while other regions use regular mesh, to ensure calculation accuracy while reducing computational load and solving time. The total transient calculation duration is set to 72 h, with the first 3 h using a 0.2 h time step to capture rapid temperature responses in the initial stage, followed by a 3 h step to improve overall calculation efficiency. The solving process adopts user-controlled tolerance of $1e^{-3}$. Furthermore, to conduct comparative analysis and result verification, the ordinary concrete wall model without PCM is calculated under the same mesh strategy and solving settings, and its

temperature response is compared with the phase change wall model.

3.2 Mesh Independence Verification

To ensure the accuracy and reliability of numerical simulation results, this study conducted model mesh independence verification tests combined with the variation characteristics of indoor temperature under external environmental temperature fluctuations. Specific verification results are shown in Fig. 13 Analysis results show that in the ordinary wall model, temperature curves for 86×10³ and 124×10³ meshes almost coincide. In the phase change wall model, temperature responses for 246×10³ meshes and above show no significant differences. This result indicates that further increasing mesh numbers has limited effect on improving calculation result accuracy. Based on this, to ensure calculation accuracy while considering calculation efficiency, this study finally selected mesh configurations of 86×10³ and 246×10³ mesh units for ordinary walls and phase change walls respectively for subsequent numerical simulation calculations.

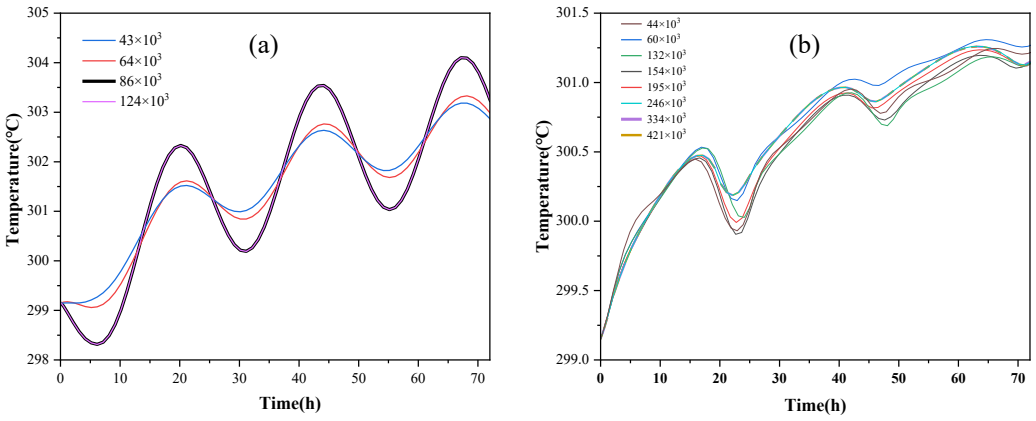


Fig. 13. Temperature response curves for mesh independence verification (a)Ordinary wall; (b)Phase change wall

3.3 Temperature Curves of Simulated Building

The simulated temperature variation curves are shown in Fig. 14. Compared with the ordinary wall, the PCM wall exhibits lower mean wall temperature, as well as lower indoor mean, maximum, and minimum temperatures, with reduced fluctuation amplitudes and gentler rates of change. This improvement originates from the latent heat absorption and release during solid–liquid phase transitions, which retard heat ingress during heating, slow down heat release during cooling, and thus create a thermal buffering effect that significantly attenuates external disturbances, demonstrating outstanding peak-shaving, thermal-lag, and temperature-stabilizing performance.

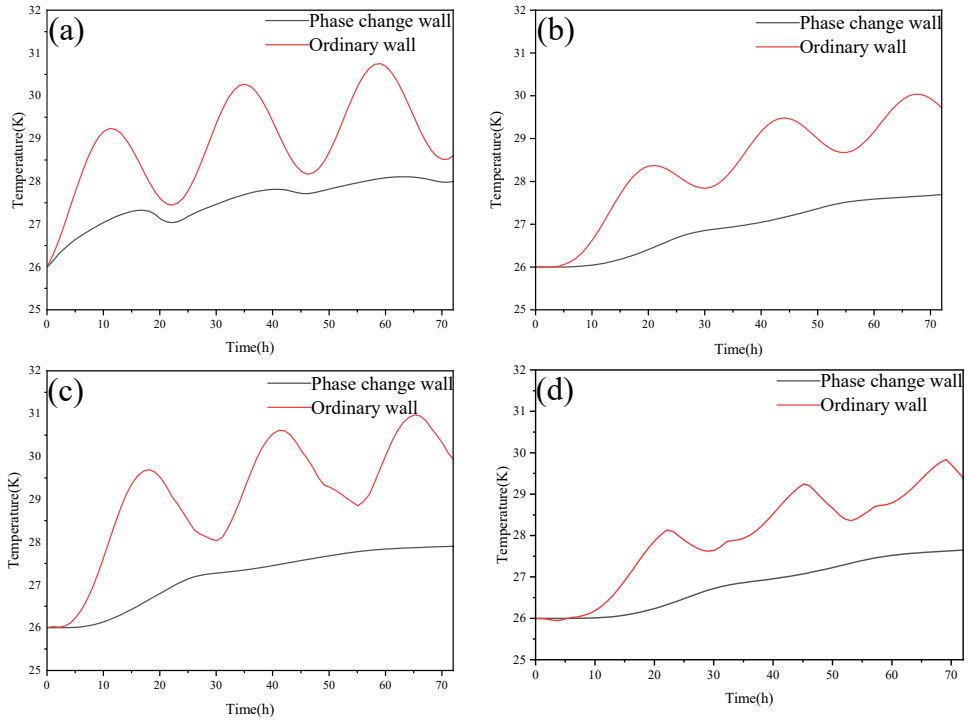


Fig. 14. Comparison of temperature variation curves of the phase change wall and ordinary wall during the 72 h transient heat transfer process: (a) average wall temperature; (b) average indoor temperature; (c) maximum indoor temperature; (d) minimum indoor temperature

3.4 Temperature Contour Analysis of Simulated Building

Based on the COMSOL simulation results, temperature data at various time steps were exported and processed to generate the temperature contours of the building model, which intuitively illustrate the spatial distribution of the indoor and outdoor temperature fields.To deeply investigate the temperature control effects of phase change concrete walls, this study selected three representative moments from simulation results for focused comparative analysis: 24 h, 30 h, and 42 h. These three moments correspond to the median, maximum, and minimum values of external environmental temperature respectively, and can comprehensively reflect the typical thermal response characteristics of the model building during a complete temperature cycle.

As shown in Fig. 15, at the median ambient temperature, the ordinary wall already exhibits pronounced high-temperature accumulation at the exterior surface and corners, with a steep temperature gradient, whereas the PCM-integrated wall maintains a uniformly distributed temperature field and indoor air temperature essentially within the comfort zone. This indicates that the PCM layer, through latent heat absorption at the early heating stage, restrains the propagation of thermal peaks into the interior, acting as an initial thermal buffer.

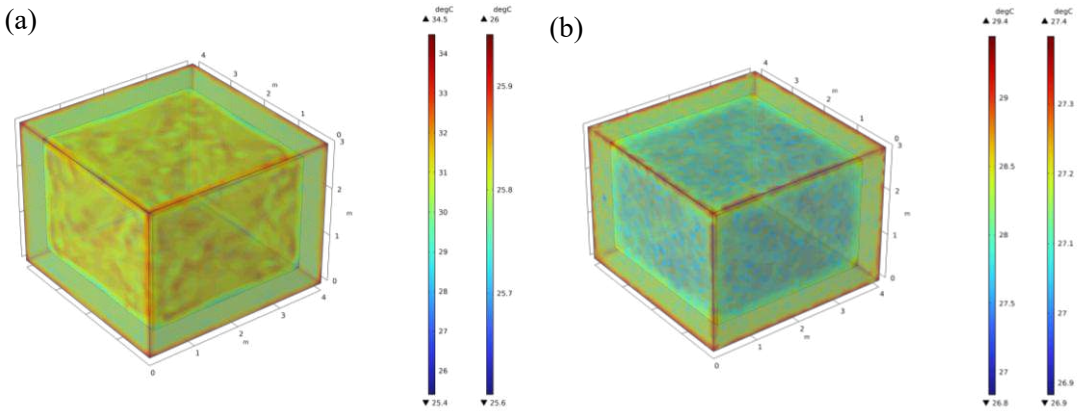


Fig. 15. Temperature field contour of the building model with (a) ordinary wall (b) phase change wall at 24 h

As seen from Fig. 16, at the peak ambient temperature, the inner surface temperature of the ordinary wall is approximately 3 °C higher than that of the PCM wall, and the indoor air temperature is about 2–3 °C higher, with evident heat accumulation near the inner surface. In contrast, the PCM wall stores a substantial portion of the incoming heat as latent heat, effectively reducing the heat flux penetrating indoors and suppressing the indoor peak temperature, demonstrating the peak-shaving capability of the PCM layer under strong thermal disturbances.

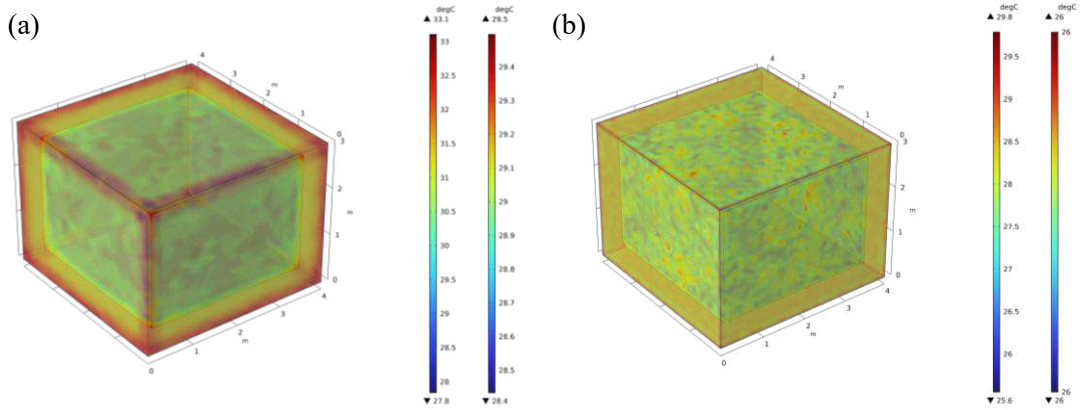


Fig. 16. Temperature field contour of the building model with (a) ordinary wall (b) phase change wall at 30 h

As illustrated in Fig. 17, at the minimum ambient temperature, the ordinary wall

still exhibits notable thermal retention, with indoor temperature approximately 1.5–2.0 °C higher than that of the PCM wall, and its cooling process is sluggish. The PCM wall, however, releases the stored latent heat gradually during solidification, resulting in a smoother temperature decay and avoiding sharp fluctuations. This reveals that the PCM layer, through delayed heat release in the cooling phase, effectively enhances the thermal inertia of the envelope and stabilizes the indoor thermal environment.

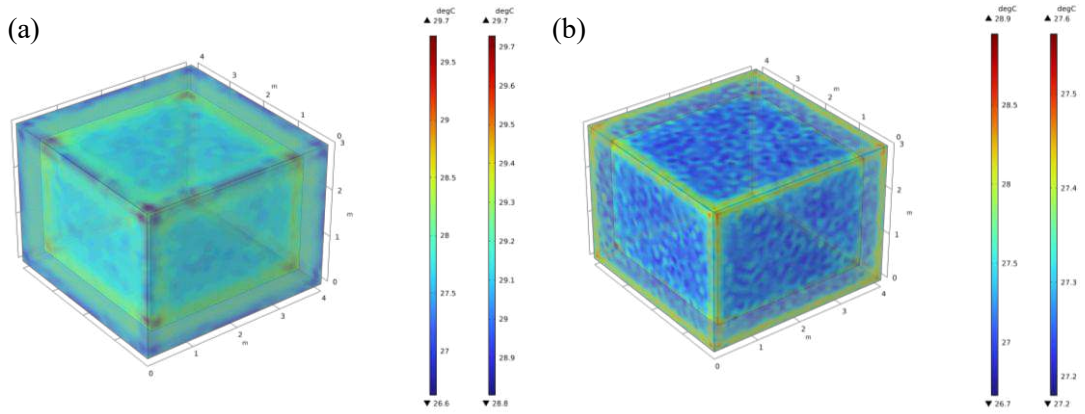


Fig. 17. Temperature field contour of the building model with (a) ordinary wall (b) phase change wall at 42 h

Comprehensive comparative analysis of temperature contours at these three typical moments shows that ordinary walls are prone to rapid heating, local high-temperature accumulation, and delayed cooling during external temperature cycle changes, with relatively sensitive responses to external thermal disturbances. In contrast, phase change walls always exhibit lower overall temperature levels and more uniform indoor temperature distribution, with significant temperature control performance advantages. Especially during external high-temperature periods, phase change walls have the most prominent suppression effects on indoor temperature peaks, effectively avoiding indoor high-temperature accumulation. During external temperature drop

periods, they have good delay and buffering effects on heat release processes, maintaining indoor temperature stability. The above results indicate that phase change gypsum walls can effectively weaken the transmission of external thermal disturbances to the indoor environment through phase change latent heat storage effects, reduce indoor temperature fluctuation amplitudes, and improve the thermal stability of building envelopes, thereby demonstrating excellent temperature control effects. This temperature control advantage can reduce building dependence on air conditioning and other cooling equipment, lower building energy consumption, and provide important support for energy conservation and emission reduction in the building field.

4 Results and Discussion

This study prepared sandwich-type phase change gypsum boards with palmitic acid–lauric acid eutectic system as the functional layer using the sandwich method. Through experimental testing and COMSOL numerical simulation, their thermal regulation performance, temperature response patterns, and indoor thermal environment optimization effects were systematically studied. Specific conclusions are as follows:

1) Heat transfer performance test results show that sandwich-type phase change gypsum boards have obvious peak-shaving, delay, and slow-release effects. During heating, the indoor-side temperature peak decreased from 32.43 °C to 31.17 °C, a reduction of 1.26 °C; the inner wall-side peak decreased from 39.90 °C to 34.91 °C, a reduction of 4.99 °C. Meanwhile, peak occurrence times were significantly delayed,

and temperature changes during the cooling stage were more gradual, indicating that the phase change layer can perform temporal regulation of heat through latent heat absorption and release, thereby slowing heat transfer toward the indoor environment. Thermal lag tests further show that the peak occurrence time of phase change gypsum boards is delayed by approximately 81 min compared with ordinary gypsum boards, reflecting significantly enhanced wall thermal inertia.

2) In terms of numerical simulation, transient heat transfer models for phase change walls and ordinary walls were established based on COMSOL Multiphysics, and 72 h heat transfer process analysis was completed. Simulation results are consistent with experimental trends. Under external periodic temperature fluctuations, phase change walls demonstrate lower overall temperature levels, smaller fluctuation amplitudes, and more uniform indoor temperature field distribution. Especially during high-temperature periods, the suppression effect on indoor temperature peaks is more pronounced.

In summary, this study verifies from both experimental and numerical simulation perspectives the good peak-shaving valley-filling, delayed heat transfer, and room temperature stabilization capabilities of sandwich-type phase change gypsum boards, which can effectively improve the thermal stability of envelopes and provide basis for their application in building energy-saving walls.

References

[1] N.N. Myint, M. Shafique, X. Zhou, Z. Zheng, Net zero carbon buildings: A review on recent advances, knowledge gaps and research directions, Case Studies in Construction Materials 22 (2025). https://doi.org/10.1016/j.cscm.2024.e04200.

[2] Y. Guan, C. Hu, X. Meng, Formation analysis of cooling load from envelopes under air-conditioning intermittent operation, Solar Energy 292 (2025). https://doi.org/10.1016/j.solener.2025.113428.

[3] M. Emam, A. Hamada, H.A. Refaey, M. Moawed, M.A. Abdelrahman, M.R. Rashed, Year-round experimental analysis of a water-based PVT-PCM hybrid system: Comprehensive 4E assessments, Renewable Energy 226 (2024). https://doi.org/10.1016/j.renene.2024.120354.

[4] T. Brudermueller, U. Potthoff, E. Fleisch, F. Wortmann, T. Staake, Estimation of energy efficiency of heat pumps in residential buildings using real operation data, Nature Communications 16(1) (2025). https://doi.org/10.1038/s41467-025-58014-y.

[5] N. Es-sakali, J. Pfafferott, M.O. Mghazli, M. Cherkaoui, Towards climate-responsive net zero energy rural schools: A multi-objective passive design optimization with bio-based insulations, shading, and roof vegetation, Sustainable Cities and Society 120 (2025). https://doi.org/10.1016/j.scs.2025.106142.

[6] O. Yatzkan, R. Cohen, E. Yaniv, O. Rotem-Mindali, Urban Energy Transitions: A Systematic Review, Land 14(3) (2025). https://doi.org/10.3390/land14030566.

[7] M. Lachheb, Z. Younsi, N. Youssef, S. Bouadila, Enhancing building energy efficiency and thermal performance with PCM-Integrated brick walls: A comprehensive review, Building and Environment 256 (2024). https://doi.org/10.1016/j.buildenv.2024.111476.

[8] A. Kasaeian, L. Bahrami, F. Pourfayaz, E. Khodabandeh, W.-M. Yan, Experimental studies on the applications of PCMs and nano-PCMs in buildings: A critical review, Energy and Buildings 154 (2017) 96-112. https://doi.org/10.1016/j.enbuild.2017.08.037.

[9] Y. Zhao, P. Zhang, Y. Qiu, Q. Li, H. Yan, Z. Wang, C. Wu, Highly conductive solid-solid phase change composites and devices enhanced by aligned graphite networks for solar/electro-thermal energy storage, Decarbon 5 (2024). https://doi.org/10.1016/j.decarb.2024.100051.

[10] J. Liu, W. Zhong, Z. Lv, C. Li, Y. Liu, Thermal management in EV wireless charging: Breakthroughs, challenges, and next-generation cooling strategies, Decarbon 10 (2025). https://doi.org/10.1016/j.decarb.2025.100133.

[11] A. Zhang, Y. Xiong, Y. Zhao, Y. Wu, Q. Xu, Y. Ding, A review of passive building thermal management with phase-change materials, Renewable & Sustainable Energy Reviews 211 (2025). https://doi.org/10.1016/j.rser.2025.115334.

[12] S.R. Leite da Cunha, J.L. Barroso de Aguiar, Phase change materials and energy efficiency of buildings: A review of knowledge, Journal of Energy Storage 27 (2020). https://doi.org/10.1016/j.est.2019.101083.

[13] Z. Chai, M. Fang, X. Min, Composite phase-change materials for photo-thermal conversion and energy storage:A review, Nano Energy 124 (2024). https://doi.org/10.1016/j.nanoen.2024.109437.
[14] C. Suresh, T.K. Hotta, S.K. Saha, Phase change material incorporation techniques in building envelopes for enhancing the building thermal Comfort-A review, Energy and Buildings 268 (2022). https://doi.org/10.1016/j.enbuild.2022.112225.
[15] K.W. Shah, P.J. Ong, M.H. Chua, S.H.G. Toh, J.J.C. Lee, X.Y.D. Soo, Z.M. Png, R. Ji, J. Xu, Q. Zhu, Application of phase change materials in building components and the use of nanotechnology for its improvement, Energy and Buildings 262 (2022). https://doi.org/10.1016/j.enbuild.2022.112018.
[16] D. Liu, J. Liang, Y. Wang, Numerical simulation on anti-freezing performance of PCM-Clay in core wall during winter construction, Applied Thermal Engineering 215 (2022). https://doi.org/10.1016/j.applthermaleng.2022.118951.
[17] V.V. Tyagi, K. Chopra, B. Kalidasan, A. Chauhan, U. Stritih, S. Anand, A.K. Pandey, A. Sari, R. Kothari, Phase change material based advance solar thermal energy storage systems for building heating and cooling applications: A prospective research approach, Sustainable Energy Technologies and Assessments 47 (2021). https://doi.org/10.1016/j.seta.2021.101318.
[18] A. Lyden, C.S. Brown, I. Kolo, G. Falcone, D. Friedrich, Seasonal thermal energy storage in smart energy systems: District-level applications and modelling approaches, Renewable & Sustainable Energy Reviews 167 (2022). https://doi.org/10.1016/j.rser.2022.112760.
[19] L. Bartela, J. Ochmann, S. Waniczek, M. Lutynski, G. Smolnik, S. Rulik, Evaluation of the energy potential of an adiabatic compressed air energy storage system based on a novel thermal energy storage system in a post mining shaft, Journal of Energy Storage 54 (2022). https://doi.org/10.1016/j.est.2022.105282.
[20] S. Zhang, Y. Yan, Evaluation of discharging performance of molten salt/ceramic foam composite phase change material in a shell-and-tube latent heat thermal energy storage unit, Renewable Energy 198 (2022) 1210-1223. https://doi.org/10.1016/j.renene.2022.08.124.
[21] Y.P. Chandra, T. Matuska, Energy modeling of thermal energy storage (TES) using intelligent stream processing system, Energy Reports 8 (2022) 1321-1335. https://doi.org/10.1016/j.egyr.2022.08.012.
[22] M. Berger, B. Schroeteler, H. Sperle, P. Puentener, T. Felder, Assessment of residential scale renewable heating solutions with thermal energy storages, Energy 244 (2022). https://doi.org/10.1016/j.energy.2021.122618.
[23] M.F. Junaid, Z.U. Rehman, M. Cekon, J. Curpek, R. Farooq, H. Cui, I. Khan, Inorganic phase change materials in thermal energy storage: A review on perspectives and technological advances in building applications, Energy and Buildings 252 (2021). https://doi.org/10.1016/j.enbuild.2021.111443.
[24] X. Huang, C. Zhu, Y. Lin, G. Fang, Thermal properties and applications of microencapsulated PCM for thermal energy storage: A review, Applied Thermal Engineering 147 (2019) 841-855. https://doi.org/10.1016/j.applthermaleng.2018.11.007.

[25] F.B. Errebai, S. Chikh, L. Derradji, M. Amara, Z. Younsi, Optimum mass percentage of microencapsulated PCM mixed with gypsum for improved latent heat storage, Journal of Energy Storage 33 (2021). https://doi.org/10.1016/j.est.2020.101910.
[26] M. Karkri, M. Lachheb, F. Albouchi, S. Ben Nasrallah, I. Krupa, Thermal properties of smart microencapsulated paraffin/plaster composites for the thermal regulation of buildings, Energy and Buildings 88 (2015) 183-192. https://doi.org/10.1016/j.enbuild.2014.11.068.
[27] M. Sheikholeslami, H.R.A. Al-Hussein, Analyzing efficiency of solar heat storage unit within a building including trombe wall equipped with phase change material in existence of fins, Journal of Building Engineering 71 (2023). https://doi.org/10.1016/j.jobe.2023.106406.
[28] P.K.S. Rathore, N.K. Gupta, D. Yadav, S.K. Shukla, S. Kaul, Thermal performance of the building envelope integrated with phase change material for thermal energy storage: an updated review, Sustainable Cities and Society 79 (2022). https://doi.org/10.1016/j.scs.2022.103690.
[29] C. Li, X. Wen, W. Cai, H. Yu, D. Liu, Phase change material for passive cooling in building envelopes: A comprehensive review, Journal of Building Engineering 65 (2023). https://doi.org/10.1016/j.jobe.2022.105763.
[30] Q. Al-Yasiri, M. Szabo, Incorporation of phase change materials into building envelope for thermal comfort and energy saving: A comprehensive analysis, Journal of Building Engineering 36 (2021). https://doi.org/10.1016/j.jobe.2020.102122.
[31] A. Laaouatni, N. Martaj, R. Bennacer, M. Lachi, M. El Omari, M. El Ganaoui, Thermal building control using active ventilated block integrating phase change material, Energy and Buildings 187 (2019) 50-63. https://doi.org/10.1016/j.enbuild.2019.01.024.
[32] Z. Luo, X. Liu, Q. Yang, Z. Qu, H. Xu, D. Xu, Numerical study on performance of porous brick roof using phase change material with night ventilation, Energy and Buildings 286 (2023). https://doi.org/10.1016/j.enbuild.2023.112972.
[33] S. Shaik, C. Arumugam, S.V. Shaik, M. Arici, A. Afzal, Z. Ma, Strategic design of PCM integrated burnt clay bricks: Potential for cost-cutting measures for air conditioning and carbon dioxide extenuation, Journal of Cleaner Production 375 (2022). https://doi.org/10.1016/j.jclepro.2022.134077.
[34] Y. Hamidi, Z. Aketouane, M. Malha, D. Bruneau, A. Bah, R. Goiffon, Integrating PCM into hollow brick walls: Toward energy conservation in Mediterranean regions, Energy and Buildings 248 (2021). https://doi.org/10.1016/j.enbuild.2021.111214.
[35] Q. Al-Yasiri, M. Szabo, Experimental study of PCM-enhanced building envelope towards energy-saving and decarbonisation in a severe hot climate, Energy and Buildings 279 (2023). https://doi.org/10.1016/j.enbuild.2022.112680.
[36] A.C. Rai, Energy performance of phase change materials integrated into brick masonry walls for cooling load management in residential buildings, Building and Environment 199 (2021). https://doi.org/10.1016/j.buildenv.2021.107930.
[37] M. Javidan, M. Asgari, M. Gholinia, M. Nozari, A. Asgari, D.D. Ganji, Thermal energy storage inside the chamber with a brick wall using the phase change process of

paraffinic materials: A numerical simulation, Theoretical and Applied Mechanics Letters 12(3) (2022). https://doi.org/10.1016/j.taml.2022.100329.
[38] C. Jia, X. Geng, F. Liu, Y. Gao, Thermal behavior improvement of hollow sintered bricks integrated with both thermal insulation material (TIM) and Phase-Change Material (PCM), Case Studies in Thermal Engineering 25 (2021). https://doi.org/10.1016/j.csite.2021.100938.
[39] H.M. Abbas, J.M. Jalil, S.T. Ahmed, Experimental and numerical investigation of PCM capsules as insulation materials inserted into a hollow brick wall, Energy and Buildings 246 (2021). https://doi.org/10.1016/j.enbuild.2021.111127.
[40] X. Jin, M.A. Medina, X. Zhang, Numerical analysis for the optimal location of a thin PCM layer in frame walls, Applied Thermal Engineering 103 (2016) 1057-1063. https://doi.org/10.1016/j.applthermaleng.2016.04.056.
[41] D. Feng, P. Li, Y. Feng, Y. Yan, X. Zhang, Using mesoporous carbon to pack polyethylene glycol as a shape-stabilized phase change material with excellent energy storage capacity and thermal conductivity, Microporous and Mesoporous Materials 310 (2021). https://doi.org/10.1016/j.micromeso.2020.110631.
[42] M. Kabdrakhmanova, S.A. Memon, A. Saurbayeva, Implementation of the panel data regression analysis in PCM integrated buildings located in a humid subtropical climate, Energy 237 (2021). https://doi.org/10.1016/j.energy.2021.121651.
[43] J. Tao, J. Luan, Y. Liu, D. Qu, Z. Yan, X. Ke, Technology development and application prospects of organic-based phase change materials: An overview, Renewable & Sustainable Energy Reviews 159 (2022). https://doi.org/10.1016/j.rser.2022.112175.
[44] M.M. Umair, Y. Zhang, K. Iqbal, S. Zhang, B. Tang, Novel strategies and supporting materials applied to shape-stabilize organic phase change materials for thermal energy storage-A review, Applied Energy 235 (2019) 846-873. https://doi.org/10.1016/j.apenergy.2018.11.017.

Supplementary Files

This is a list of supplementary files associated with this preprint. Click to download.

- Table.docx